NONLOCAL INTEGRAL-EQUATION APPROXIMATIONS:

II. LENNARD-JONES FLUIDS

Yaoqi Zhou[1] and George Stell[2]

[1]*Department of Chemistry, State University of New York at Stony Brook, Stony Brook, NY 11794.*

[2]*Departments of Chemistry and Mechanical Engineering, State University of New York at Stony Brook, Stony Brook, NY 11794.*

September 29, 1989

SUSB College of Engineering Report # 558 (September 1989)

ABSTRACT

The zeroth order (hydrostatic) nonlocal integral-equation approximation is applied here to Lennard-Jones (LJ) fluids. Systems of homogeneous LJ fluids are investigated, as well as LJ fluids near a hard wall, a model CO_2 wall, and inside two model CO_2 walls. The hydrostatic hypernetted chain (HHNC) approximation is shown to be better than both the Percus-Yevick and the hypernetted chain approximations when compared with computer simulations. The phenomena of solid wetting by liquid, solid wetting by gas, and capillary condensation are predicted by the HHNC approximation.

I. INTRODUCTION

The wetting transition for a solid-gas interface is a transition from partial wetting to complete wetting of the solid surface by a liquid.[1] The capability of predicting this phenomena has been a crucial test for various theories of inhomogeneous systems. Commonly used integral equations, such as the hypernetted-chain (HNC) approximation and the Percus-Yevick (PY) approximation, seem to fail this test.[2] Although attempts have been made to account for the wetting phenomena by using improved integral equations,[3] until now one has had to rely mainly on density functional theories applied to free-energy functionals.[4–5] Since there is little knowledge concerning exact free-energy functionals for realistic pair potentials, the construction of approximate free-energy functionals has been typically based on hard-sphere free energy functionals with mean-field approximations for the attractive-potential contribution[6–9] or has been restricted to hard-sphere systems.[10] The former theories are hampered by a treatment of attractive forces that is lacking in quantitative accuracy as well as having some other drawbacks.[11,12] In our treatment here, the attractive forces are not separated from the repulsive ones—they are treated on the same level of approximation. The treatment is initiated on the level of a two-point description rather than a thermodynamic one, so there is no need to make an **a priori** guess as to the functional form of the free-energy functional. Instead one truncates a systematic density-functional expansion of the direct correlation function. Compared with free-energy functionals, direct correlation functions reflect the structure of a molecular system in a much more detailed way. As a result, a density-functional expansion of direct correlation functions[13–19] seems to be a promising new approach.

In a previous paper[20] introducing nonlocal corrections to standard integral-equation approximations (e.g. HNC and PY),[13–19] we formulated a hydrostatic Percus-Yevick (HPY) approximation and a hydrostatic hypernetted chain (HHNC) approximation, which are zeroth-order nonlocal density-functional theories. Using a simple step weight function, we applied these hydrostatic approximations to the

homogeneous hard-sphere fluid, hard spheres near a wall, and to hard spheres inside a slit pore.[20] The HHNC approximation was shown to be an improvement over the HNC approximation in all the cases we considered. We also showed that the new approximations are capable of accounting for wetting transitions in a sense that the standard HNC and PY approximation are not.[20]

The purpose of this paper is to apply the HHNC approximation to a Lennard-Jones (LJ) fluid. (The HPY will not be used here since it was found to overcorrect the PY approximation in preliminary computations done by us.[20]) Homogeneous LJ fluids and LJ fluids near a wall are investigated in Section II and in Section III, respectively. Both the phenomena of a CO_2 solid wetting by liquid and a hard wall wetting by gas are found. In Section IV, we investigate LJ fluids inside two model CO_2 walls. The capillary condensation is predicted by the HHNC approximation. All results appear to be in good agreement with computer-simulation data. However, our current techniques for numerically solving our equations do not yield the wetting temperature and surface critical temperature with high precision. The extent to which precision can be improved by the use of more accurate algorithms is not yet clear to us, and we regard our results as exploratory. In this paper, we heavily lean on the development and notation already introduced in ref.20, which is the first paper of this series.

II. THE HOMOGENEOUS LENNARD-JONES FLUID

For an one-component homogeneous system, we have the Ornstein-Zernike (OZ) equation

$$h - c = \rho h * c \tag{2.1}$$

with the HHNC closure[20] [(2.16a) of ref.20]

$$g(r) = \exp[-\beta u(r) + h(r) - c(r) - b(r)] \tag{2.2}$$

$$b(r) = \beta[\mu^{ex}|_{\rho^*(r)} - \mu^{ex} - \rho h^*(r)\frac{\partial \mu^{ex}}{\partial \rho}] \tag{2.3}$$

where $h(r)$ and $c(r)$ are the pair correlation function and direct pair correlation function respectively, $*$ denotes a three dimensional convolution integral, $T = 1/\beta k_B$ is the temperature, $u(r)$ is the pair potential, $b(r)$ is an approximate bridge function, $\mu^{ex} = \mu - \mu^{id}$ is the part of the chemical potential excess to the ideal gas chemical potential, and $\rho^*(r)$ is a weighted nonlocal density, $\rho^*(r) = \rho[h^*(r) + 1]$. Here, the weighted pair correlation function, $h^*(r)$, is given by

$$h^*(r) = \int h(r')w(|\mathbf{r} - \mathbf{r}'|)d\mathbf{r}' \ . \tag{2.4}$$

The $w(r)$ is a weight function which satisfies the normalization condition

$$\int w(r)d\mathbf{r} = 1 \tag{2.5}$$

For a Lennard-Jones fluid, we have the pair potential

$$\beta u(r) = 4[(\sigma/r)^{12} - (\sigma/r)^6]/T^* \tag{2.6}$$

with the reduced temperature

$$T^* = k_B T/\epsilon \tag{2.7}$$

where ϵ and σ are parameters in units of energy and distance respectively.

One choice of weight function, which was discussed earlier,[20,21] is

$$w(r) = \frac{f(r)}{\int f(r)d\mathbf{r}} \tag{2.8}$$

where f is a Mayer-f function. This is appropriate to a hard-sphere fluid, but not to a Lennard-Jones fluid, since in general one wants a weight function such that $w(r) \geq 0$, in order to avoid the possibility of negative effective density $\rho^*(r)$ for some r. Therefore, we use

$$w(r) = \frac{F(r)}{\int F(r)d\mathbf{r}} \tag{2.9}$$

with

$$F(r) = e^{-\beta U(r)} - 1 \tag{2.10}$$

$$\begin{aligned} \beta U(r) &= 4[(\sigma/r)^{12} - (\sigma/r)^6]/T^* + 1/T^*, \quad r/\sigma < 2^{1/6} \\ &= 0, \quad r/\sigma > 2^{1/6} \end{aligned} \tag{2.11}$$

Although this weight function, which is associated with the repulsive part of the LJ potential, is a natural one to use here, at this stage of our computations its use is essentially exploratory. Other choices may well improve our quantitative results and we intend to systematically pursue this point in future work. In this connection we note that we have as yet made no attempt to introduce self-consistency into our scheme in the sense of using a weight function such that the thermodynamics of our system obtained from the $g(r)$ of our integral equation matches our chemical-potential input in a homogeneous system. Instead we simply input an accurate expression for the chemical potential of an LJ fluid. Such an expression can be obtained from the equation of state of Nicolas et. al. (NGST),[22] which fits computer simulation data[23,24] very accurately. We use this equation of state as input here. Detailed expressions can be found in Appendix A.

Eqs. (2.1-2.3) form a closed set of equations for the HHNC approximation, which can be solved by a simple iterative method.[18,19] One can also solve these equations by combining Newton-Raphson and Picard methods. However, we find that one such method developed by Labík et. al.[25] does not work very well for the HHNC approximation at a high density or a low temperature although it does work better than simple iterative methods for the PY and HNC approximations.

In Fig.1 the radial distribution function obtained by the HHNC approximation is compared with the PY approximation, the HNC approximation and a computer simulation.[24] Results show that the HHNC approximation are better than both the PY and HNC approximations. In Fig.2 the cavity function $y(r) = g(r)\exp(\beta u)$ according to various approximations is also plotted.

III. LENNARD-JONES FLUIDS NEAR A WALL

For a system of fluids near a planar wall, we have, in the HHNC approximation,[20]

$$\begin{aligned} h(z) - c(z) &= \rho^B \int c^B(|\mathbf{r} - \mathbf{r}'|) h(z') d\mathbf{r}' \\ &= \rho^B \int h^B(|\mathbf{r} - \mathbf{r}'|) c(z') d\mathbf{r}' \end{aligned} \tag{3.1}$$

$$\ln g(z) = -\beta V^{ext}(z) + h(z) - c(z) - b(z) \ . \tag{3.2}$$

with the bridge function

$$b(z) = \beta[\mu^{ex}|_{\rho^*(z)} - \mu^{ex} - \rho^B h^*(z)\frac{\partial \mu^{ex}}{\partial \rho^B}] \tag{3.3}$$

where a superscript B denotes the bulk homogeneous properties, $c(z)$ is direct correlation function, $h(z) = g(z) - 1 = \rho(z)/\rho^B - 1$ with the density profile $\rho(z)$ and bulk density ρ^B, $V^{ext}(z)$ is the interaction potential between a fluid particle and the wall, and $\rho^*(z) = \rho^B[h^*(z) + 1]$ with

$$h^*(z) = \int w(|\mathbf{r}' - \mathbf{r}|)h(z')d\mathbf{r}' \ . \tag{3.4}$$

Both the weight function and chemical potential here are the same as those used in the previous section.

For LJ fluids near a hard wall, we have

$$\begin{aligned} V^{ext}(z) &= 0, \quad z > 0 \\ &= \infty, \quad z < 0 \end{aligned} \tag{3.5}$$

while for LJ fluids near a model CO_2 solid wall, we use, following ref. 4

$$\begin{aligned} V^{ext}(z) = V_{CO_2}(z) &= 4\pi\epsilon_w\rho_w\sigma_w^3[\frac{1}{45}(\sigma_w/z)^9 - \frac{1}{6}(\sigma_w/z)^3], \quad z > 0 \\ &= \infty, \quad z < 0 \end{aligned} \tag{3.6}$$

where $\epsilon_w/k_B = 153\text{K}$, $\sigma_w = 3.727\text{Å}$, and $\rho_w\sigma_w^3 = 0.988$.

Eqs.(3.1)-(3.3) can be solved by a simple iterative method which is described elsewhere.[19,20] A simple description is also given in Appendix B.

In Fig.3 and Fig.4, it can be seen that the HHNC results are in a good agreement with computer simulations for LJ fluids near the model CO_2 wall.[26] In Fig.5, density profiles for LJ fluids near the CO_2 wall predicted by the HHNC approximation are shown at various temperatures with a fixed bulk density $\rho^B\sigma^3 = 0.08$. As the temperature decreases, a thick liquid film near the surface appears to be built up. However, the figure suggests that the HHNC gives too strong oscillations at temperatures near the coexistence temperature. The coverage Γ is defined as

$$\Gamma = \rho^B \int_0^\infty h(z)dz \ . \tag{3.7}$$

When approaching the complete wetting transition at constant pressure, one has $\Gamma \approx |T - T_{coex}|^{-\beta_s}$ with $\beta_s = 0$ for short-range potential ($\Gamma \approx \ln|T - T_{coex}|$) and $\beta_s = 1/3$ for a LJ fluid.[27] Fig.6 shows the logarithm of coverage Γ predicted by the HHNC approximation. (The range of $T - T_{coex}$ shown is too limited and too far from $T = T_{coex}$ to permit a reliable estimate of β_s in our approximation). Here, in obtaining the density profile near a CO_2 wall, the bulk correlations for LJ gases are obtained from the PY approximation.

It is difficult for us to precisely calculate the wetting temperature and surface critical temperature using our current techniques because we can not be certain of the cause of divergent numerical solutions. They can be due to transitions but are also likely to arise from numerical problems. Calculating the density profile along the coexistence curve for LJ gases near a model CO_2 solid, we find a divergent solution when $T^* \geq 1.0$. For $T^* < 1.0$, a finite value of Γ is obtained. ($\Gamma = 0.466$ when $T^* = 0.99$, $\rho^B\sigma^3 = 0.0258$). Therefore, the wetting temperature T_w^* given by the HHNC approximation appears to be 1.0 or more.

In Fig.7, the result for LJ liquids near a hard wall is shown. At the reduced temperature $T^* = 1.25$ and reduced density $\rho^B\sigma^3 = 0.6$ (the coexisting densities at this temperature are $\rho^B\sigma^3 = 0.56$ for liquid and $\rho^B\sigma^3 = 0.11$ for gas), wetting of the hard wall by gas is predicted by the HHNC approximation. Both the HNC and PY approximations give very different results from the HHNC prediction. The hard-wall wetting by gas has been observed in computer simulations[28] and in a density-functional theory[7b] for truncated LJ fluids. In Fig.8, the bridge function for the above system is shown.

In obtaining the density profile near a hard wall, a CO_2 wall, and in the calculations below, the bulk correlation function for the LJ liquid is calculated from the modified HNC (MHNC) approximation,[29] except at gas densities, where we use the PY approximation instead, because of its very high accuracy at such densities.

IV. LENNARD-JONES FLUIDS INSIDE A SLIT PORE

For fluids inside a pore, it is appropriate to deal with the distribution function $g(\mathbf{r})$ and a function $C(\mathbf{r})$ which differs from the direct correlation function $c(\mathbf{r})$ by a constant term[19]

$$C(\mathbf{r}) = c(\mathbf{r}) + a_1, \quad a_1 = 1 - \rho^B \tilde{c}^B(0) \tag{4.1}$$

The OZ equation (3.1) then can be rewritten as

$$g - C = \rho^B h^B * C = \rho^B c^B * g \ . \tag{4.2}$$

Eq.(3.2) can also be changed accordingly. Here the bulk fluid is taken to be the homogeneous system that is found when the external force for maintaining the inhomogeneity (i.e. two walls) is turned off in a grand ensemble.[19]

For LJ fluids inside two CO_2 walls, we have the external potential

$$V^{ext}(z) = V_{CO_2}(L/2 + z) + V_{CO_2}(L/2 - z) \tag{4.3}$$

where L is the distance between two walls. The origin of axes is chosen in the equal distance to walls. As a result, one has $g(z) = g(-z)$ and $C(z) = C(-z)$.

The coverage Γ for a *single* wall is defined as

$$\Gamma = \rho^B \int_0^{L/2} h(z) dz \ . \tag{4.4}$$

The numerical algorithm for solving integral equations is presented in appendix B. Fig.9 shows that density profiles predicted by the HHNC approximation at various separation of walls when the bulk fluid is an LJ gas. At a certain separation ($L/\sigma \approx 5$), the Lennard-Jones fluid seems to be crystallized. The coverage is plotted as a function of separation of walls in Fig.10. The figure indicates that there is a capillary condensation[30] near $L/\sigma = 5.65$ while the corresponding computer simulation[31] gives a capillary condensation near $L/\sigma \approx 5.25$ (Fig.10). The figure also shows that the HHNC approximation overestimates the coverage Γ, especially near transition regions. (This is not caused by the cutoff LJ interaction,

$R_c = 5.3\sigma$, in the Monte-Carlo simulation,[31] as we shall discuss in Section V below.) The PY approximation result for the coverage Γ, also shown in Fig.10, is found to be accurate only at very small and very large separations of walls when compared with simulations. In a small range of a certain separations near 5.65σ, two convergent solutions are obtained for the HHNC approximation (Fig.11). This phenomenon has previously been observed in computer simulations and density-functional theories.[32–33]

V. DISCUSSION AND SUMMARY

In this paper, the HHNC approximation is applied to homogeneous and inhomogeneous LJ fluids. It is shown that the HHNC approximation is capable of accounting for both the wetting transition and capillary condensation. In contrast, the PY approximation and HNC approximation, which are reasonably accurate for hard-spheres near a hard-wall or inside a hard pore, both fail when applied to LJ fluids, especially near transitions.

We have repeated our calculations for a fluid of particles interacting with a cut-off LJ potential with the NGST equation-of-state corrected for the cutoff as described in ref 34. For a cutoff distance 5.3σ we find that the difference between our results for the full LJ potential and the cutoff LJ potential is negligible, so we have not differentiated between these two potentials in discussing our results. The difference between the simulation and integral-equation results shown in Fig.10 is most likely mainly due to deficiencies in the HHNC approximation. (Here the simulation results are for a cutoff at 5.3σ.)

For a cutoff distance 2.5σ, the difference between the results for cutoff and full LJ potentials becomes apparent in the HHNC approximation. For example, we find a divergent solution when $T^* \geq 0.8$ along the coexistence curve for the cutoff LJ gases. ($\Gamma = 0.33$ when $T^* = 0.79$ and $\rho^B\sigma^3 = 0.00952$). In comparison, the simulation predicts the wetting temperature $T_w^* = 0.84$. [34]

Some advantages of our approach were already noted in our Introduction. In the version we present here there are some disadvantages, too. We have not found a way to obtain surface tension as easily as in standard density function theory based on explicit use of a free-energy functional. Thus we currently have no convenient and accurate way of monitering that important quantity. (This adds to the difficulty of locating the critical point.[35]) As has been shown elsewhere, the HHNC approximation does not satisfy the contact theorem for hard-spheres near a hard wall.[20] For this reason, one would not expect to predict the solvation force due to the walls very accurately from our approach in considering fluids in slit pores. More generally, the version of our approach presented here lacks the guarantee of self-consistency in all thermodynamic quantities that is bulit into a direct approximation of the free energy. All in all, however, we find the exploratory results of the paper extremely encouraging.

ACKNOWLEDGMENTS

We are indebted to Dr. P. Monson and Dr. R. Evans for many helpful discussions and Dr. A. Malijevský for conveying to us his programs, which use the numerical algorithm developed by him and his coworkers for a one-component uniform fluid in the PY and HNC approximations. This work was supported by the National Science Foundation.

APPENDIX A: THE EXCESS CHEMICAL POTENTIAL FOR A HOMOGENEOUS LJ FLUID

The chemical potential can be obtained from the thermodynamic relation

$$\rho \frac{\partial \mu}{\partial \rho} = \frac{\partial P}{\partial \rho} \qquad (A.1)$$

once the equation of state is known. We use the NGST equation of state for LJ fluid,[22] which fits computer-simulation data rather accurately. After a little algebra,

we obtain

$$\frac{T^* d\beta\mu^{ex}}{d\rho^*} = \sum_{n=2}^{9} nB_n(\rho^*)^{n-2} + e^{-\gamma(\rho^*)^2} \sum_{m=1}^{6} C_m[(2m+1)(\rho^*)^{2m-1} - 2\gamma(\rho^*)^{2m+1}] \tag{A.2}$$

$$T^*\beta\mu^{ex} = \sum_{n=2}^{9} \frac{n}{n-1} B_n(\rho^*)^{n-1} + \frac{1}{2} \sum_{m=1}^{6} C_m I_m \tag{A.3}$$

where

$$B_2 = x_1 T^* + x_2(T^*)^{1/2} + x_3 + x_4(T^*)^{-1} + x_5(T^*)^{-2} \tag{A.4}$$

$$B_3 = x_6 T^* + x_7 + x_8(T^*)^{-1} + x_9(T^*)^{-2} \tag{A.5}$$

$$B_4 = x_{10} T^* + x_{11} + x_{12}(T^*)^{-1} \tag{A.6}$$

$$B_5 = x_{13} \tag{A.7}$$

$$B_6 = x_{14}(T^*)^{-1} + x_{15}(T^*)^{-2} \tag{A.8}$$

$$B_7 = x_{16}(T^*)^{-1} \tag{A.9}$$

$$B_8 = x_{17}(T^*)^{-1} + x_{18}(T^*)^{-2} \tag{A.10}$$

$$B_9 = x_{19}(T^*)^{-2} \tag{A.11}$$

$$C_1 = x_{20}(T^*)^{-2} + x_{21}(T^*)^{-3} \tag{A.12}$$

$$C_2 = x_{22}(T^*)^{-2} + x_{23}(T^*)^{-4} \tag{A.13}$$

$$C_3 = x_{24}(T^*)^{-2} + x_{25}(T^*)^{-3} \tag{A.14}$$

$$C_4 = x_{26}(T^*)^{-2} + x_{27}(T^*)^{-4} \tag{A.15}$$

$$C_5 = x_{28}(T^*)^{-2} + x_{29}(T^*)^{-3} \tag{A.16}$$

$$C_6 = x_{30}(T^*)^{-2} + x_{31}(T^*)^{-3} + x_{32}(T^*)^{-4} \tag{A.17}$$

$$I_m = \int_0^{(\rho^*)^2} [(2m+1)t^{m-1} - 2\gamma t^m] e^{-\gamma t} dt \tag{A.18}$$

where $\rho^* = \rho\sigma^3$, $T^* = k_B T/\epsilon$, $\gamma = 3.0$ and the parameters x_i, $i = 1 - 32$ can be found in Table 4. of ref.22.

APPENDIX B: THE NUMERICAL METHOD

The numerical algorithm for solving integral equations for the system of LJ fluids inside a slit pore is as follows:

1. input the bulk direct correlation function c^B and initial guesses for both $\tau^{(0)}(z) \equiv g(z) - C(z)$ and $g^{(0)}(z)$.

2. calculate $g^{(n)}(z)$ by using the equation

$$g^{(n)}(z) = \exp[-\beta V^{ext}(z) + \tau^{(n-1)}(z) - b(z) - 1 + a_1] \qquad (B.1)$$

with the help of eqs.(3.3), (4.1), (2.4), (2.9), (A.2) and (A.3), where $b(z)$ is calculated from $g^{(n-1)}(z)$.

3. mix $g^{(n)}(z)$ with $g^{(n-1)}(z)$

$$g^{(n)}(z) = \alpha g^{(n)}(z) + (1-\alpha) g^{(n-1)}(z) \qquad (B.2)$$

(Near a transition, α is usually chosen as small as 0.1.)

4. calculate $\tau^{(n)}(z)$ from equation

$$\tau^{(n)}(z) = \rho^B c^B * g^{(n)} \qquad (B.3)$$

by using the 1D fast Fourier transform technique.

5. go to step 2 if $g^{(n)}(z) - g^{(n-1)}(z)$ is not small enough.

An alternative procedure is to use τ and C as intermediate iterative functions and/or to mix $\tau(z)$ instead of $g(z)$. Our numerical calculations show that the region in which one can obtain a convergent solution is significantly smaller if one uses such alternative algorithms.

When the wall-wall separation, L, increases, we have the solution for LJ fluids near a single wall. Our calculations shows that this algorithm gives better convergence than a similar algorithm designed for a single wall problem ($\tau' = h - c$ either with c or h as intermediate iterative functions).

REFERENCES

[1]. For example, D. E. Sullivan and M. M. Telo da Gama, in *Fluid Interfacial Phenomena*, edited by C. A. Croxton (Wiley, London, 1985).

[2]. R. Evans, P. Tarazona, and U. Marini Bettolo Marconi, *Mol. Phys.* **50**, 993 (1983).

[3]. E. Bruno, C. Caccamo, and P. Tarazona, *Phys. Rev. A* **35**, 1210 (1987); E. Bruno and C. Caccamo, *Phys. Rev. A* **38**, 515 (1988).

[4]. C. Ebner and W. F. Saam, *Phys. Rev. Lett.* **38**, 1486 (1977).

[5]. For example, R. Evans and P. Tarazona, *Phys. Rev. A* **28**, 1864 (1983).

[6]. S. Nordholm, M. Johnson, and B. C. Freasier, *Aust. J. Chem.* **33**, 2139 (1980); M. Johnson and S. Nordholm, *J. Chem. Phys.* **75**, 1953 (1980).

[7]. a) P. Tarazona, *Mol. Phys.* **52**, 81 (1984). b) P. Tarazona and R. Evans, *Mol. Phys.* **52**, 847 (1984).

[8]. P. Tarazona, *Phys. Rev. A* **31**, 2672 (1985).

[9]. T. F. Meister and D. M. Kroll, *Phys. Rev. A* **31**, 4055 (1985).

[10]. W. A. Curtin and N. W. Ashcroft, *Phys. Rev. A* **32**. 2909 (1985); *Phys. Rev. Lett.* **26**, 2775 (1986); A. R. Denton and N. W. Ashcroft, *Phys. Rev. A.* **39**, 426, 4701 (1989).

[11]. J. Fischer, U. Heinbuch and M. Wendland, *Mol. Phys.* **61**, 953 (1987).

[12]. R. D. Groot, J. P. van der Eerden, and N. M. Faber, *J. Chem. Phys.* **87**, 2263 (1987).

[13]. J. K. Percus, *Phys. Rev. Lett.* **8**, 462 (1962).

[14]. J. L. Lebowitz and J. K. Percus, *J. Math. Phys.* **4**, 116 (1963).

[15]. G. Stell, *Phys. Rev. Lett.* **20**, 533 (1968); G. Stell, *Phys. Rev. B* **2**, 2811 (1970).

[16]. L. Blum and G. Stell, *J. Stat. Phys.* **15**, 439 (1976).

[17]. D. Sullivan and G. Stell, *J. Chem. Phys.* **67**, 2567 (1977).

[18]. Y. Zhou and G. Stell, *J. Chem. Phys.* **89**, 7010,7020 (1988).

[19]. Y. Zhou and G. Stell, *Mol. Phys.* **66**, 767, 791 (1989).

[20]. Y. Zhou and G. Stell, to be submitted.

[21]. G. Stell, *Cluster Expansions for Classical Systems in Equilibrium*, Section 12, in *The Equilibrium Theory of Simple Fluids*, ed. by H. L. Frisch and J. L. Lebowitz (Benjamin, N.Y., 1964).

[22]. J. J. Nicolas, K. E. Gubbins, W. B. Streett, and D. J. Tildesley *Mol. Phys.* **37**, 1429 (1979).

[23]. J. A. Barker and D. Henderson, *Rev. mod. Phys.*, **48**, 587 (1976).

[24]. L. Verlet, *Phys. Rev.*, **165**, 201 (1968).

[25]. S. Labík, A. Malijevský and P. Voňka, *Mol. Phys.*, **56**, 709 (1985).

[26]. J. E. Lane, T. H. Spurling, B. C. Freasier, J. K. Perram, and E. R. Smith, *Phys. Rev. A* **20**, 2147 (1979).

[27]. R. Lipowsky, *Phys. Rev. B*, **32**, 1731 (1985).

[28]. For example, D. E. Sullivan, D. Levesque, and J. J. Weis, *J. Chem. Phys.* **72**, 1170 (1980); J. R. Henderson and F. van Swol, *Mol. Phys.* **56**, 1313 (1985).

[29]. Y. Rosenfeld and N. W. Ashcroft, *Phys. Rev. A* **20**, 1208 (1979).

[30]. R. Evans, U. Marini Bettolo Marconi and P. Tarazona, *J. Chem. Phys.* **86**, 7138 (1987); *ibid.* **84**, 2376 (1986).

[31]. J. E. Lane and T. H. Spurling *Aus. J. Chem.* **33**, 231 (1980).

[32]. See, e.g. M. Schoen, C. L. Rhykerd, Jr., J. H. Cushman, and D. J. Diestler, *Mol. Phys.* **66**, 1171 (1989); Waltan and Quirke, *Mol. Simulation*, xxxx, (1989)

[33]. See, e.g. P. Tarazona, U. Marini Bettolo Marconi and R. Evans, *Mol. Phys.*, **60**, 573 (1987); B. K. Peterson and K. E. Gubbins, *Mol. Phys.*, **62**, 215 (1987).

[34]. J. E. Finn and P. A. Monson, *Phys. Rev. A.*, **39**, 6402 (1989).

[35]. R. Evans, in *Liquids at interface*, edited by J. Charvolin, J. F. Joanny and J. Zinn-Justin (Elsevier Science Publishers B. V. 1989).

FIGURE CAPTIONS

Fig.1 The radial distribution function of the uniform LJ fluid at $T^* = 1.127$ and $\rho\sigma^3 = 0.85$. The HHNC approximation (—), HNC approximation (- - -), PY approximation (— - —), and computer simulation data[24] (•).

Fig.2 The logarithm of cavity function $y(r)[= g(r)\exp(\beta u)]$ for the uniform LJ fluid. Parameters and symbols as in Fig.1.

Fig.3 The density profile of a LJ fluid near a CO_2 wall at $T^* = 0.9$ and $\rho^B\sigma^3 = 0.0101$. a) HHNC approximation (—), HNC approximation (- - -), PY approximation (— - —). b) computer simulation.[26] For the HHNC approximation, the bulk correlation functions are obtained in the PY approximation.

Fig.4 The density profile of a LJ fluid near a CO_2 wall at $T^* = 1.1$. For bottom to top, $\rho^B\sigma^3 = 0.03, 0.04, 0.0465$. a) HHNC approximation, b) computer simulation.[26] For the HHNC approximation, the bulk correlation functions are obtained in the PY approximation. We do not show the HHNC results for $\rho^B = 0.0465$ since we can not obtain a convergent solution.

Fig.5 The density profile of a LJ fluid near a CO_2 wall at $\rho^B\sigma^3 = 0.08$ obtained by the HHNC approximation. From bottom to top $T^* = 1.5$, 1.4, 1.3, 1.25, 1.23, 1.225, 1.22.

Fig.6 The logarithm of coverage $\ln\Gamma$ as a function of $-\ln(T^* - T^*_{coex})$ at a constant bulk density $\rho^B\sigma^3 = 0.08$. The HHNC approximation (•), the PY approximation (∘). The coexistence temperature T^*_{coex} for $\rho^B\sigma^3 = 0.08$ in the NGST equation of state is 1.185

Fig.7 The density profile for a LJ liquid at $T^* = 1.25$ and $\rho^B\sigma^3 = 0.6$ near a hard wall. The bulk correlation function is obtained from the modified HNC approximation with the adjustable parameter $\eta^{PY} = 0.28$.[29] The HHNC approximation (—), the HNC approximation (- - -) and the PY approximation (— - —).

Fig.8 The bridge function obtained from the HHNC approximation for a LJ fluid near a hard wall. All parameters and symbols as in Fig.7.

Fig.9 The density profile inside two model CO_2 walls obtained in the HHNC approximation for a LJ fluid at $T^* = 1.1$ and $\rho^B\sigma^3 = 0.03$. The bulk correlation function is obtained from the PY approximation. $L/\sigma = 2$ (—), $L/sigma = 2.4$, (- - -), $L/\sigma = 3.5$ (— - —), $L/\sigma = 3.9$, (— - - —), $L/\sigma = 4.7$, (— - - - —), $L/\sigma = 6$ (— - - - - —).

Fig.10 The reduced coverage $\Gamma^* = \Gamma\sigma^2$ for a LJ fluid inside a slit pore as a function of the reduced wall separation L/σ. Other parameters as in Fig.9. The HHNC approximation (•), The PY approximation (∘), The Monte-Carlo simulation (△).[30]

Fig.11 The density profile inside two model CO_2 walls. $L/\sigma = 5.65$ Other parameters as in Fig.9. The HHNC approximation (—), The PY approximation (- - -). There appears to be two solutions for the HHNC approximation, as shown.

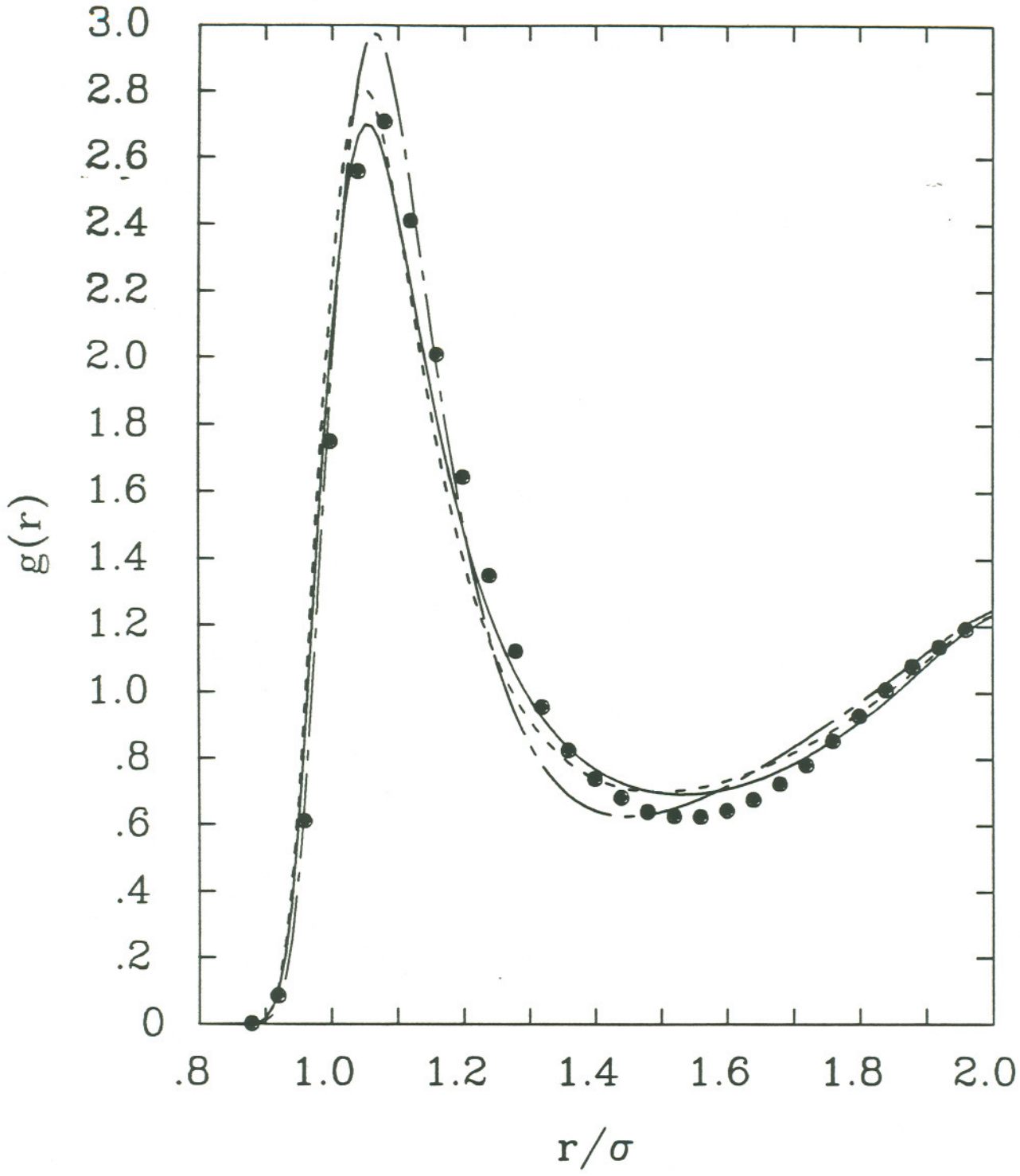
3.0
2.8
2.6
2.4
2.2
2.0
1.8
1.6
1.4
1.2
1.0
.8
.6
.4
.2
0
g(r)
.8
1.0
1.2
1.4
1.6
1.8
2.0
r/σ

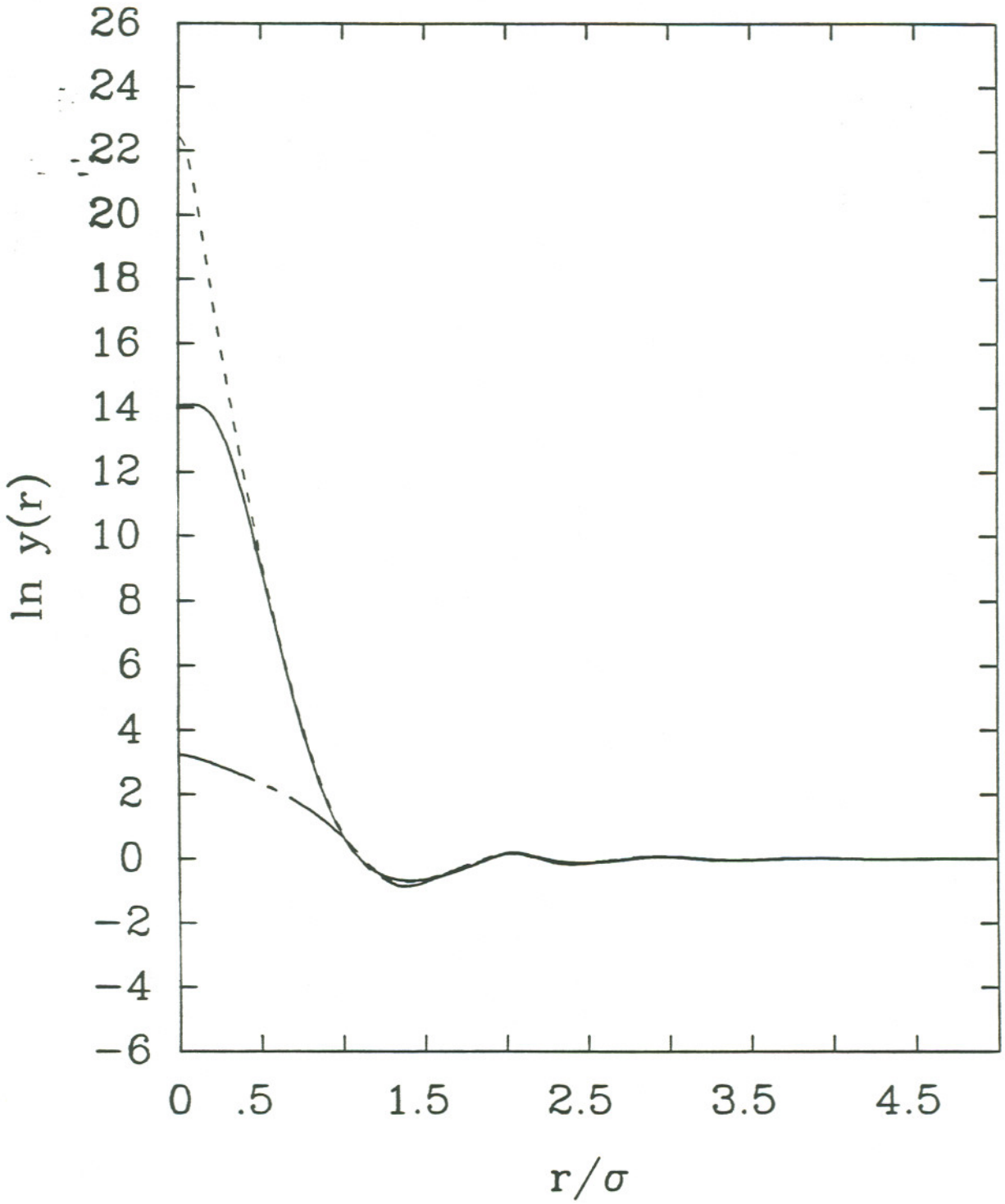
26
24
22
20
18
16
14
12
10
8
6
4
2
0
−2
−4
−6
ln y(r)
0
.5
1.5
2.5
3.5
4.5
r/σ

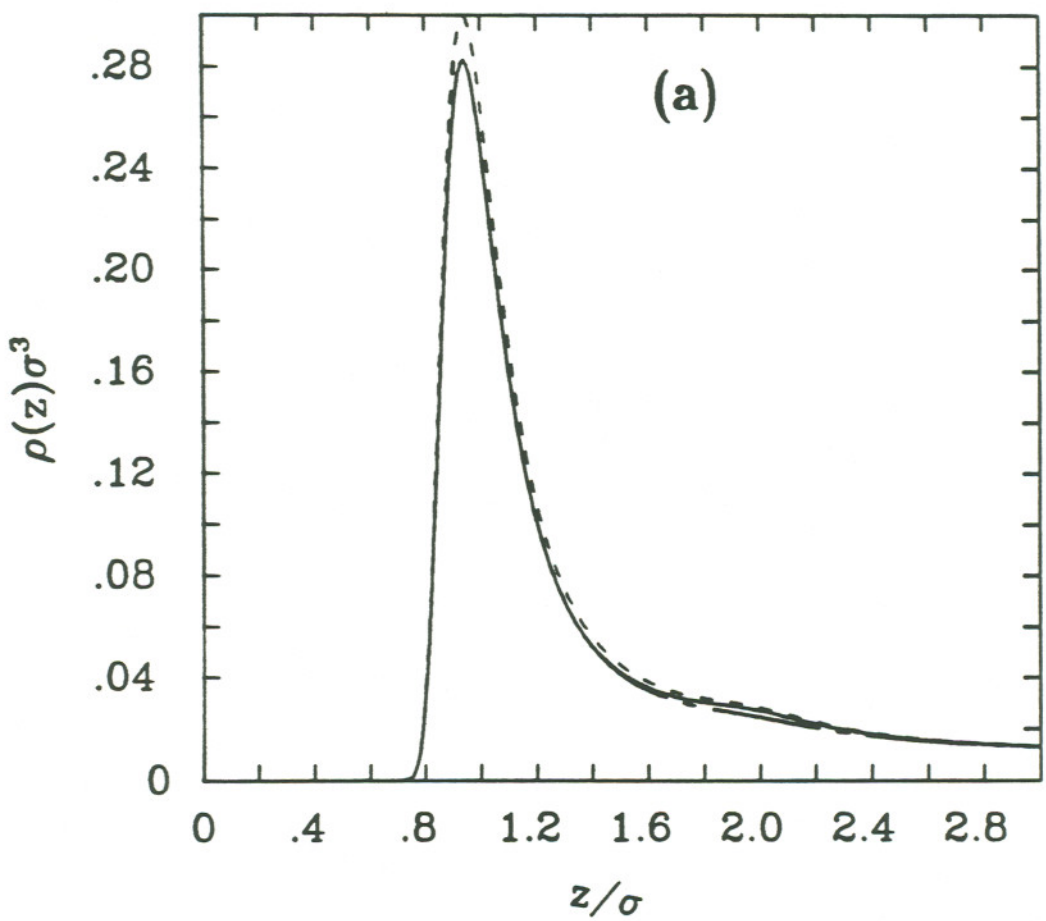
(a)
.28
.24
.20
.16
.12
.08
.04
0
$\rho(z)\sigma^3$
0
.4
.8
1.2
1.6
2.0
2.4
2.8
z/σ

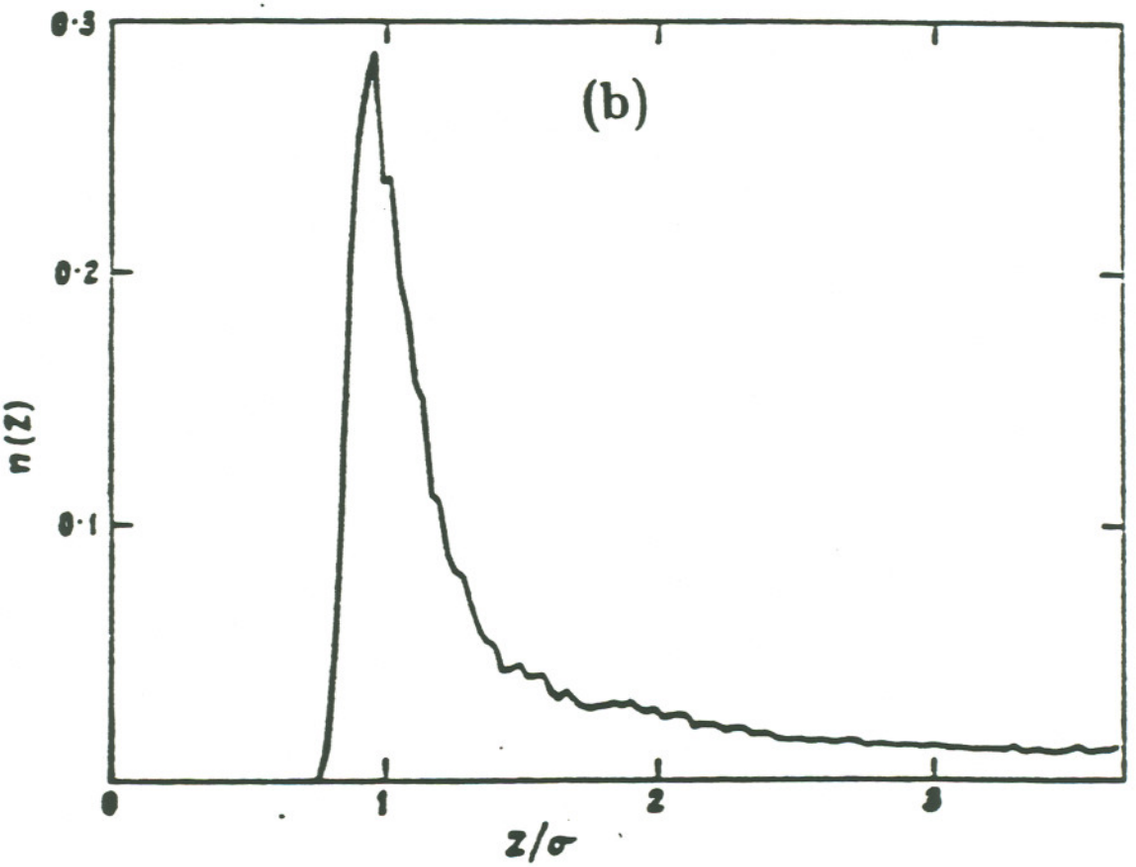

Fig 3b

Fig 3b

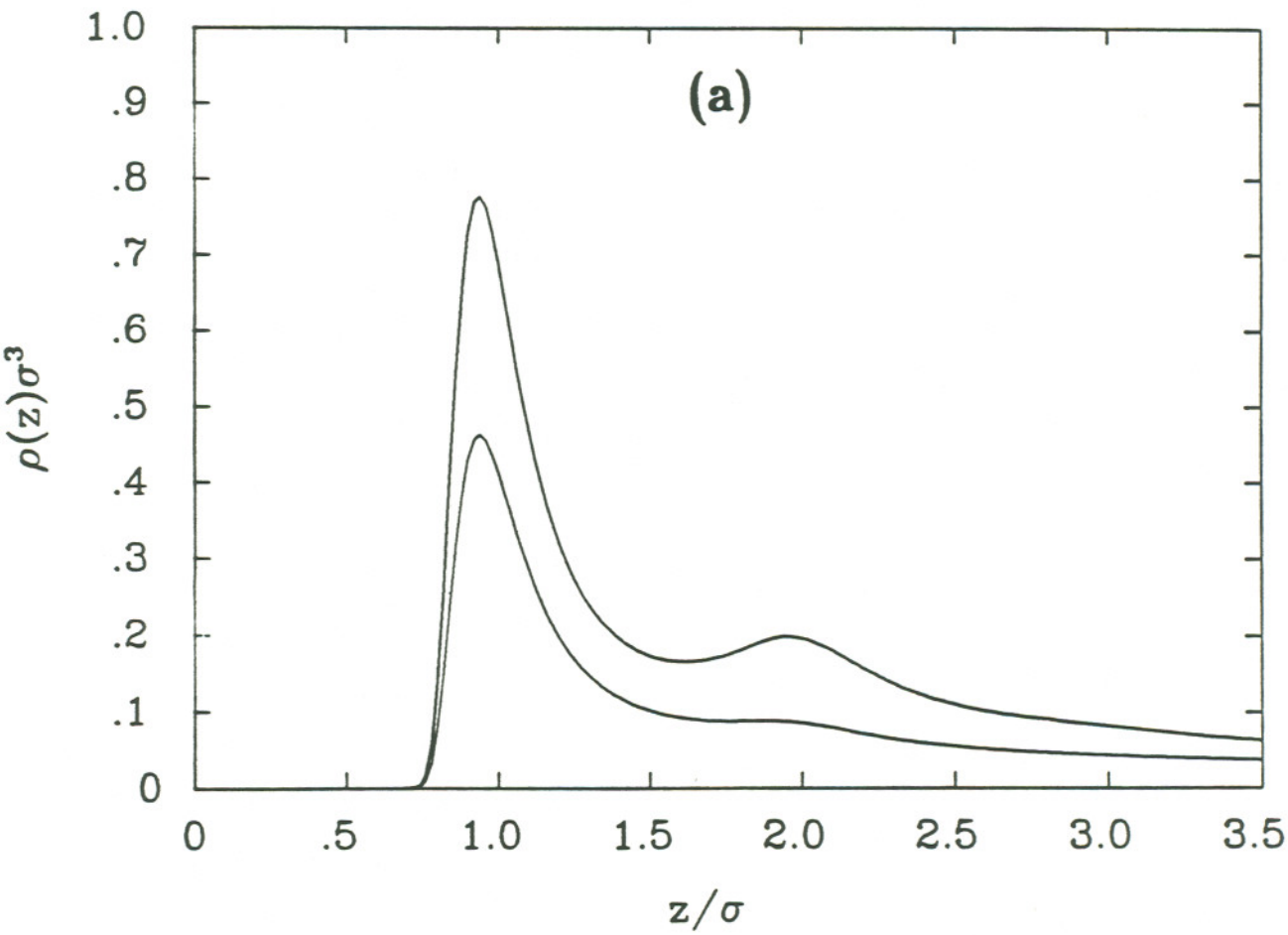

Fig 4a

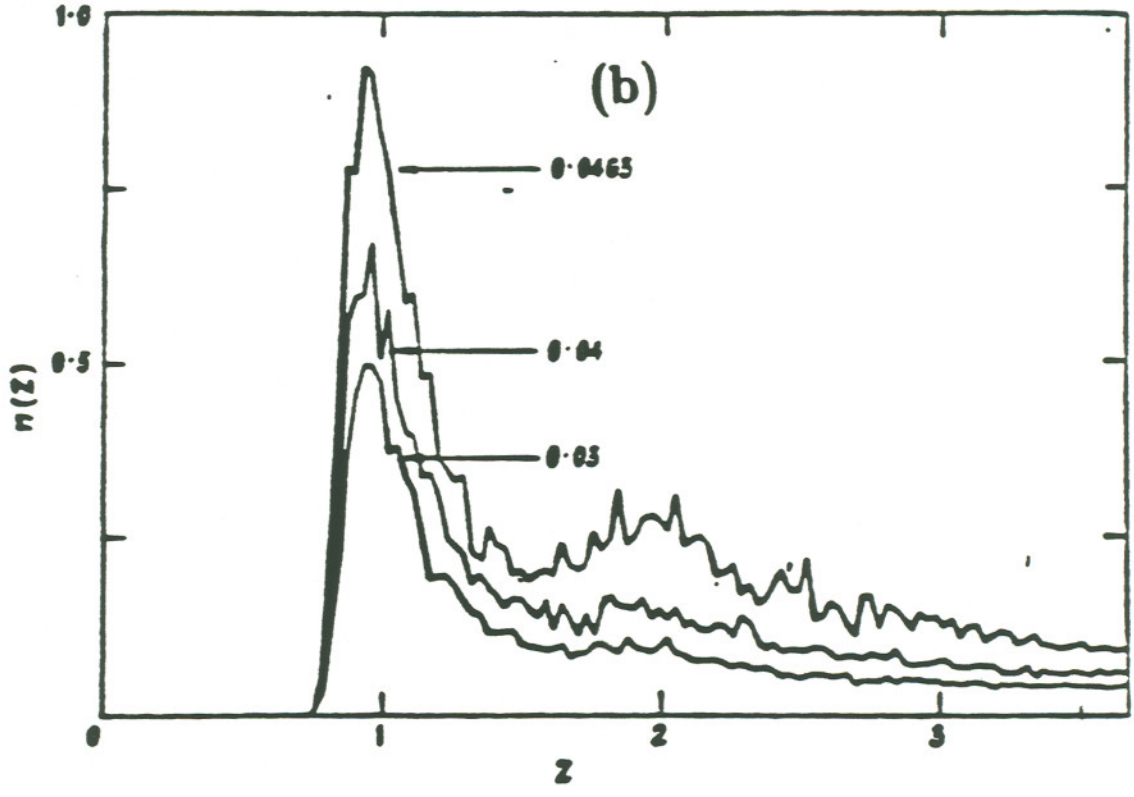
(b)
1·0
0·5
n(z)
0·0465
0·04
0·03
0
1
2
3
z

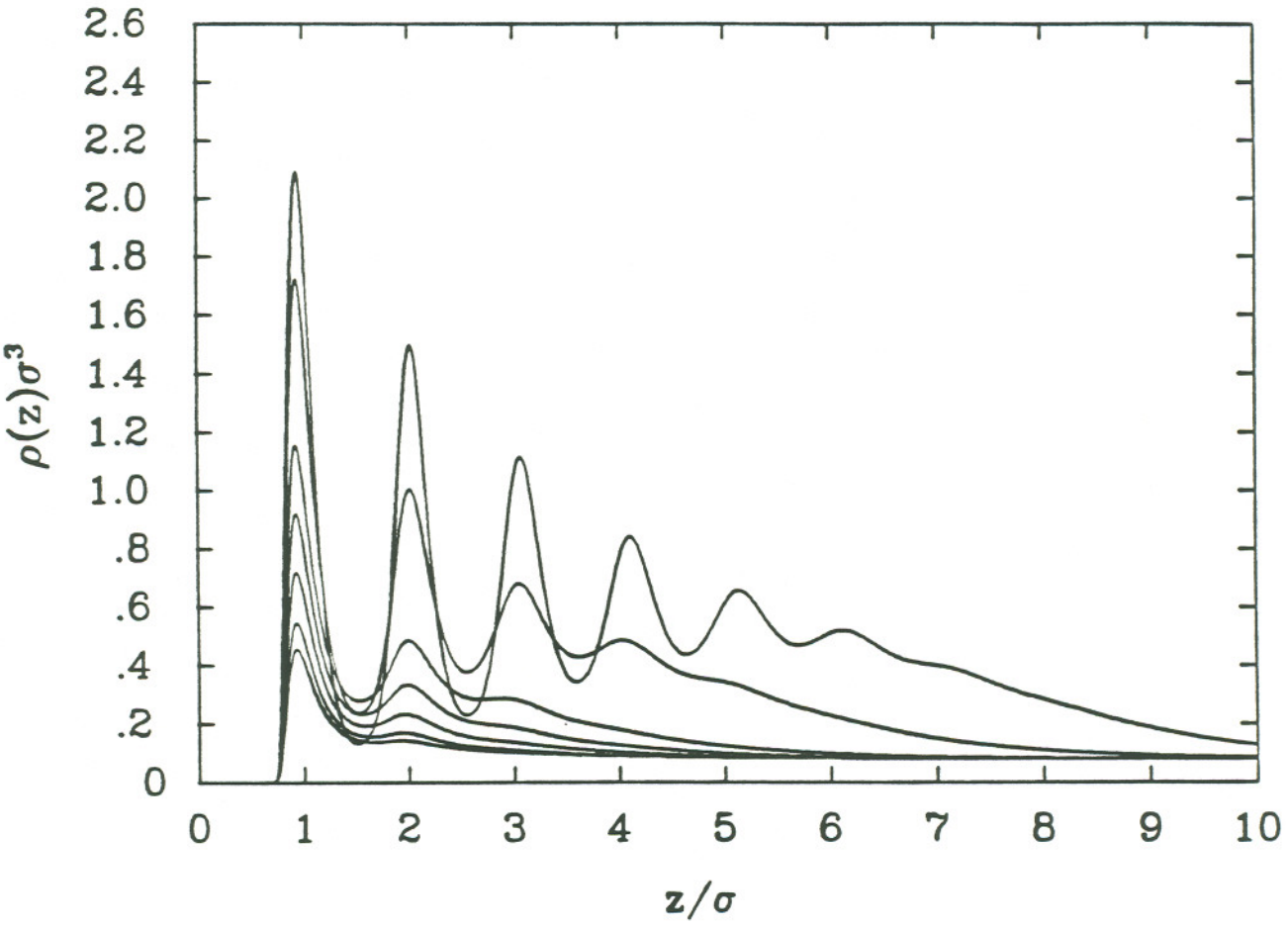

Preliminal II Fig 5

Fig 5

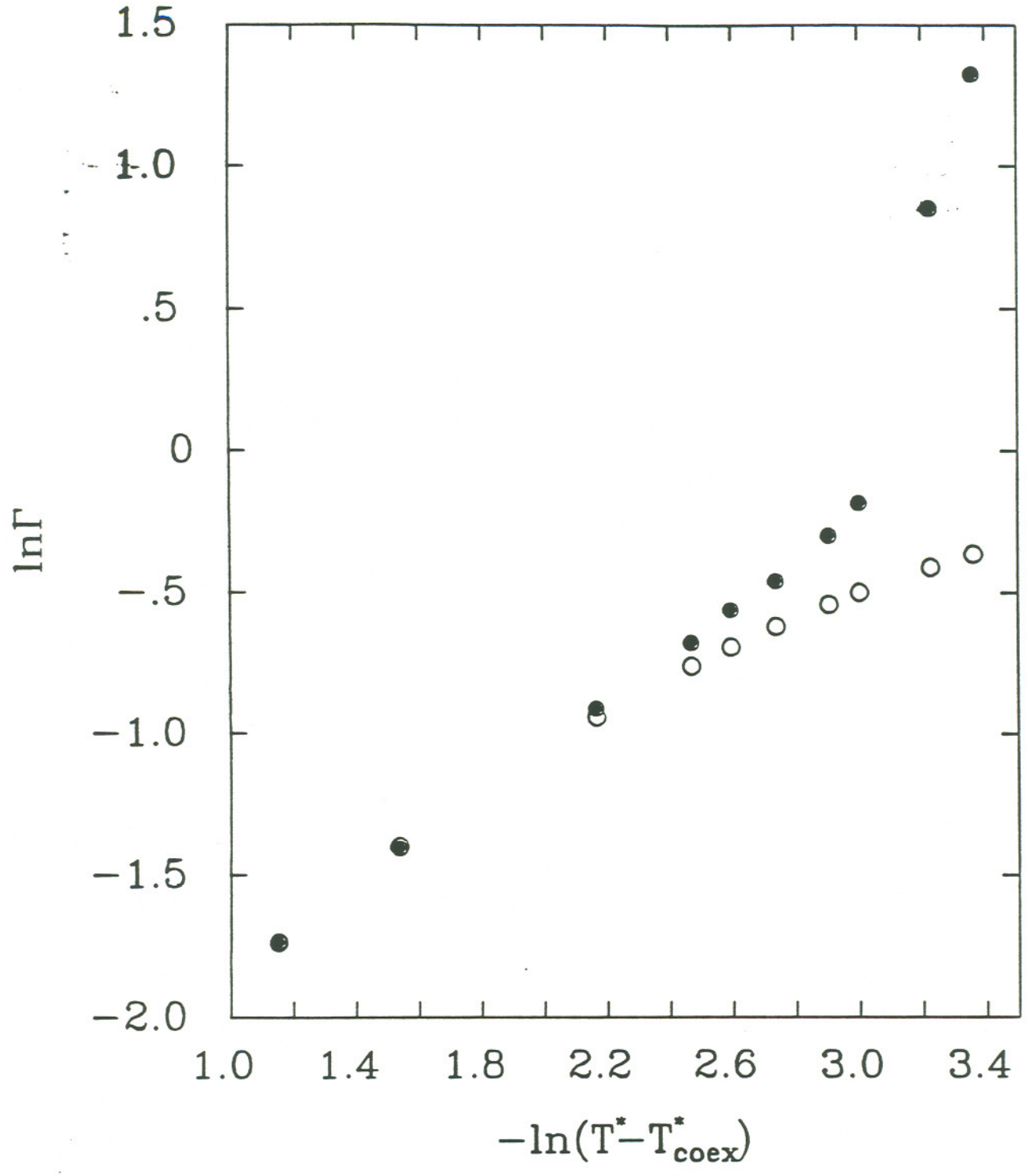

Nonideal II. Fig 6

Fig 6

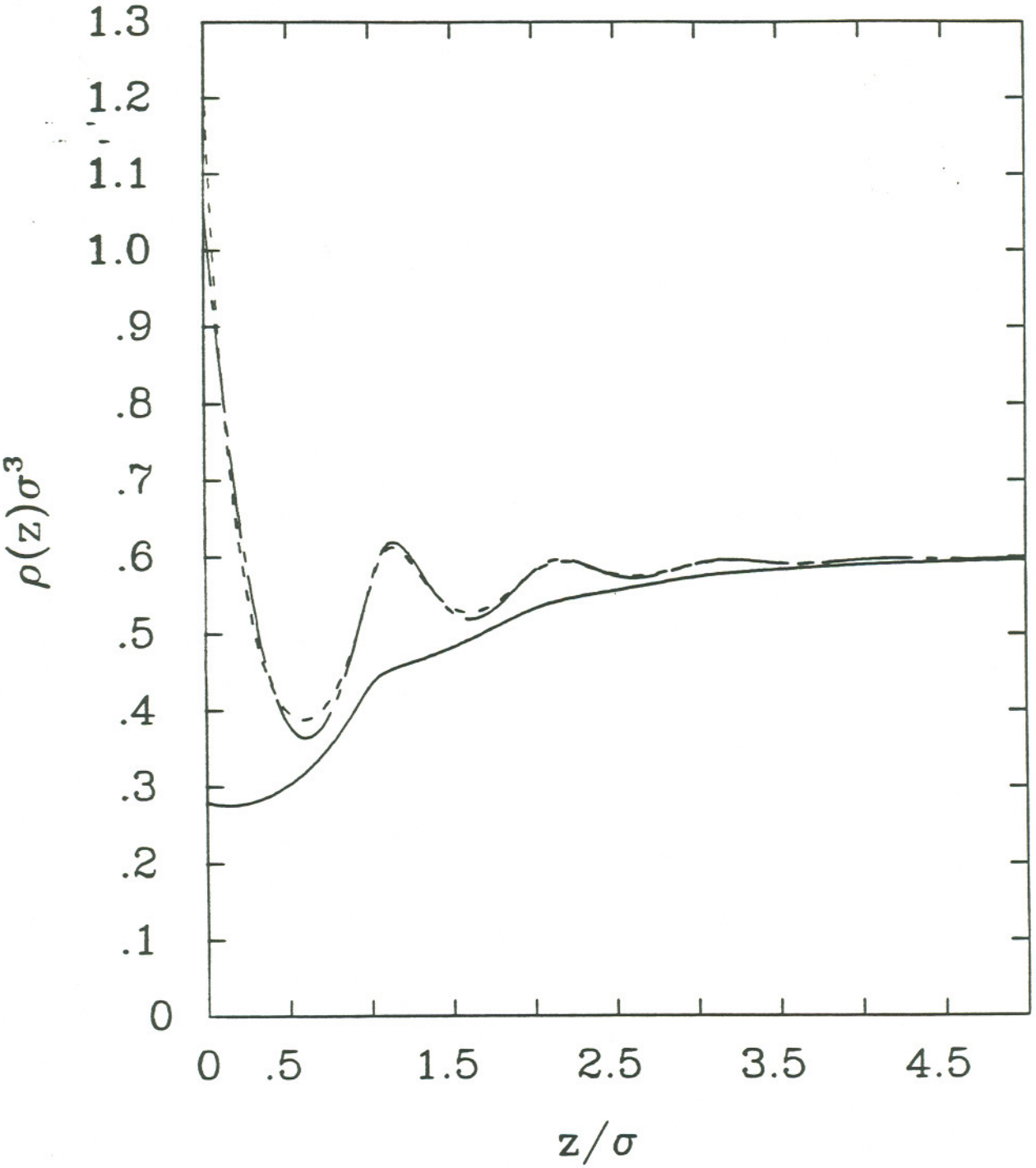
1.3
1.2
1.1
1.0
.9
.8
.7
.6
.5
.4
.3
.2
.1
0
$\rho(z)\sigma^3$
0
.5
1.5
2.5
3.5
4.5
z/σ

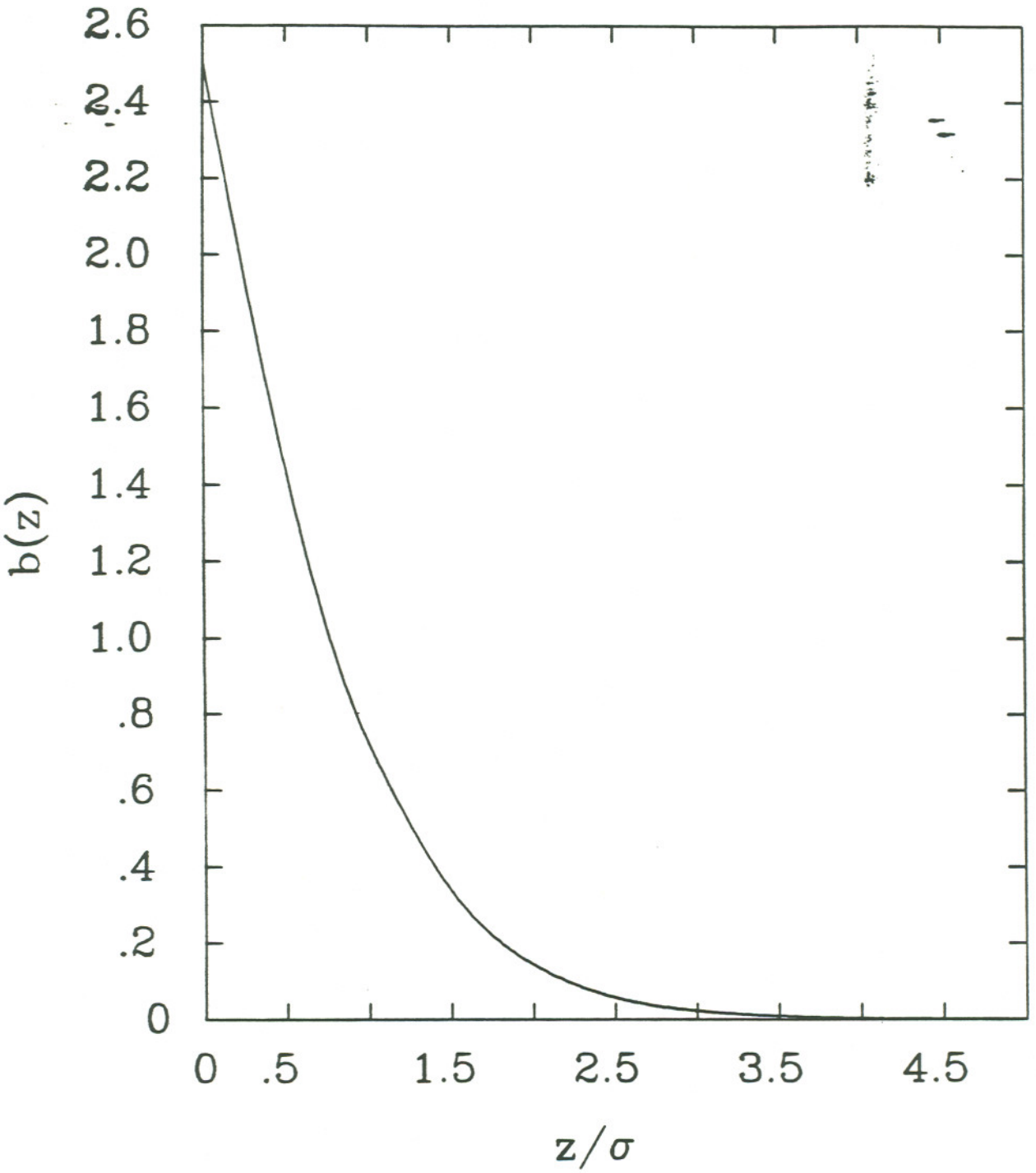
2.6
2.4
2.2
2.0
1.8
1.6
1.4
1.2
1.0
.8
.6
.4
.2
0
b(z)
0
.5
1.5
2.5
3.5
4.5
z/σ

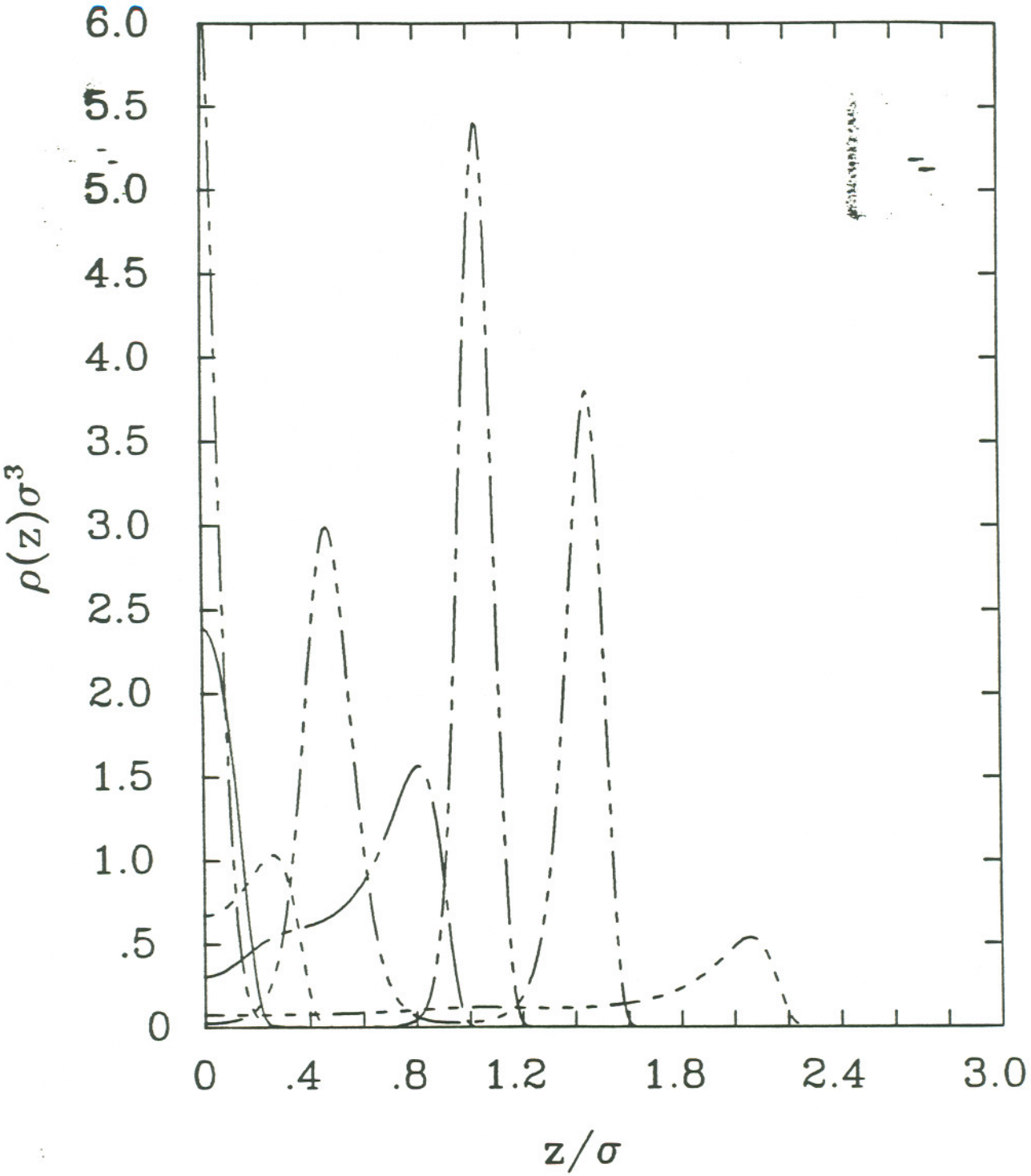
6.0
5.5
5.0
4.5
4.0
3.5
3.0
2.5
2.0
1.5
1.0
.5
0
$\rho(z)\sigma^3$
0
.4
.8
1.2
1.8
2.4
3.0
z/σ

Fig 9

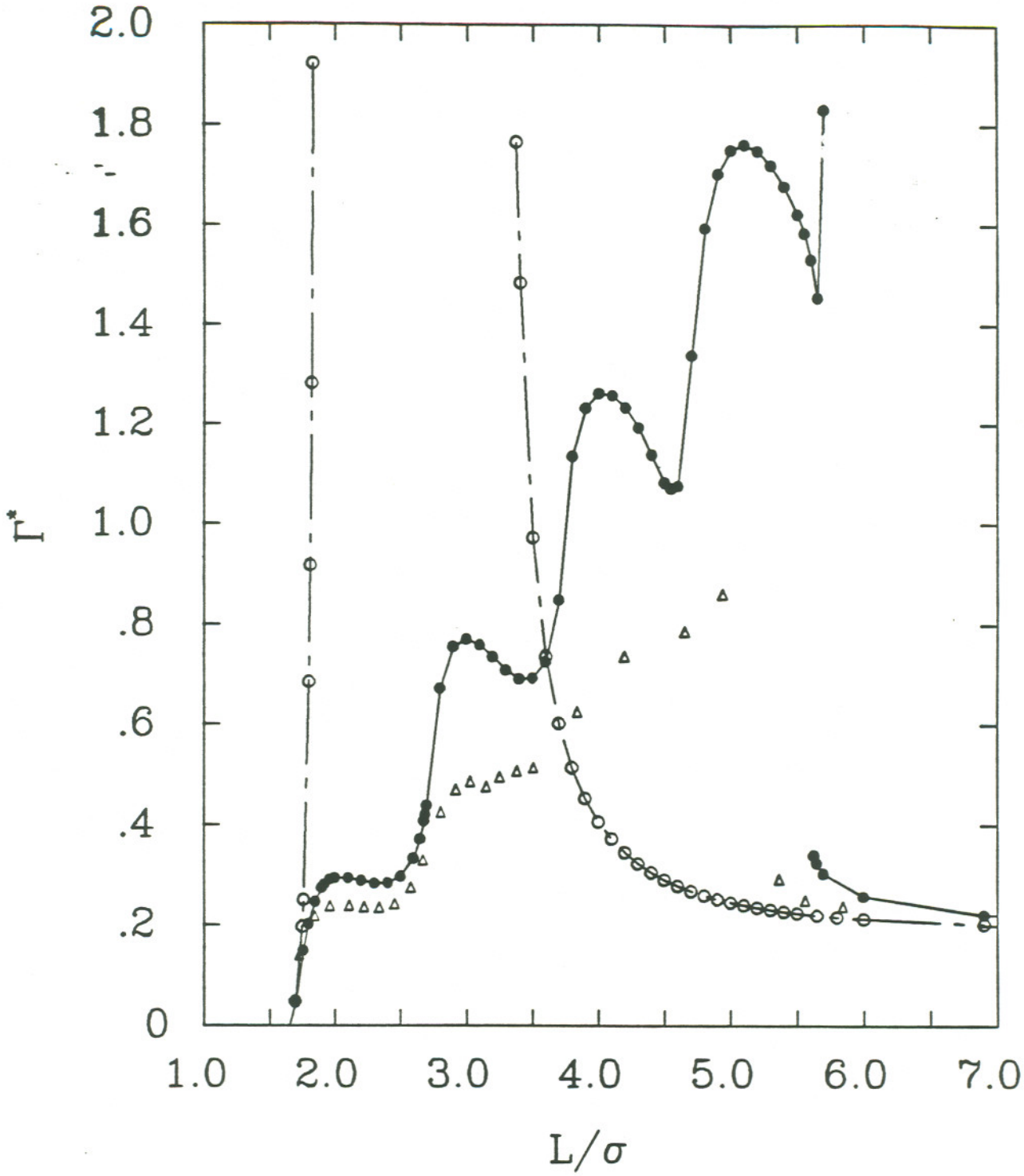

Nonlocal II Fig 10

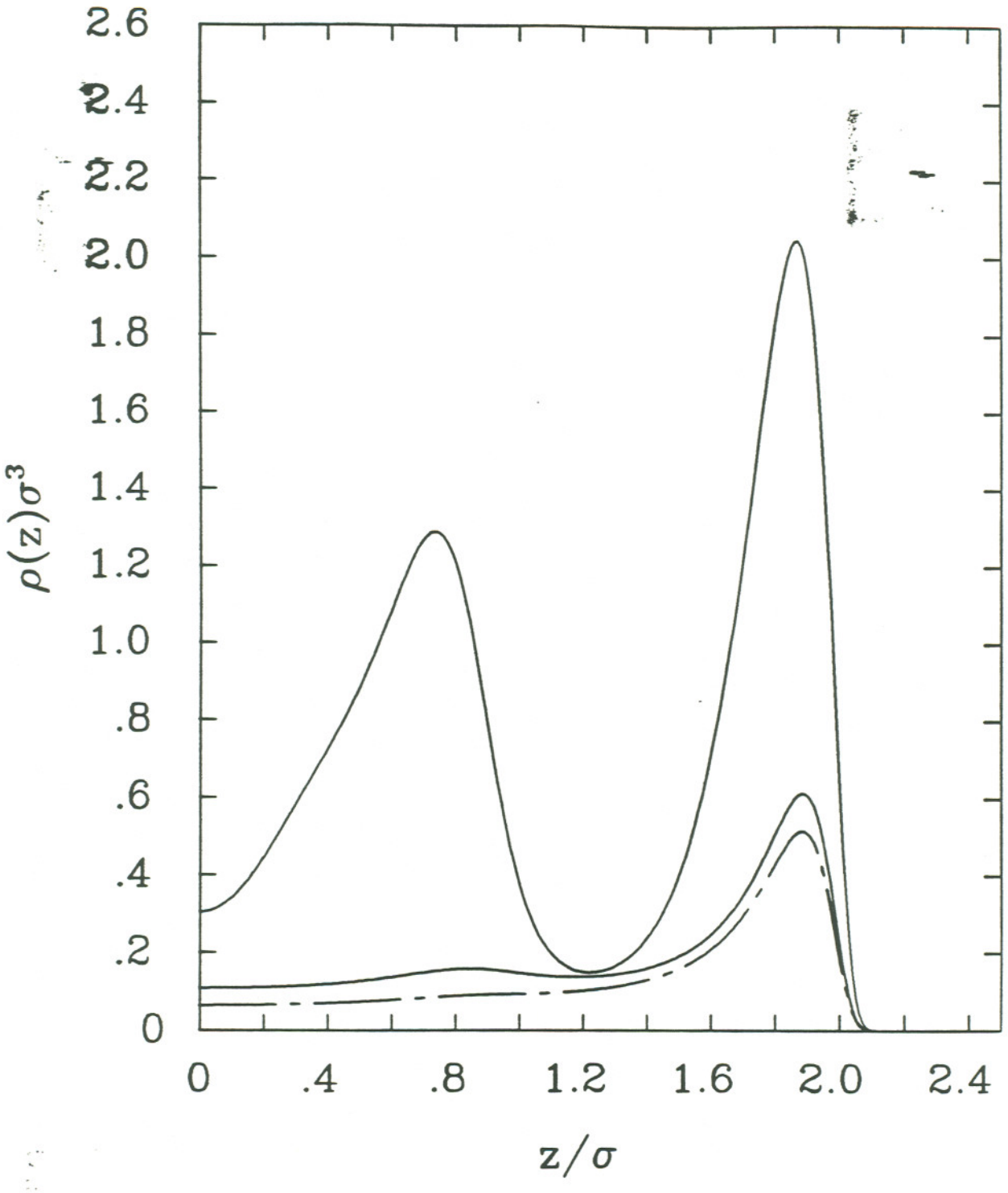
2.6
2.4
2.2
2.0
1.8
1.6
1.4
1.2
1.0
.8
.6
.4
.2
0
$\rho(z)\sigma^3$
0
.4
.8
1.2
1.6
2.0
2.4
z/σ

Fig. 11